Organometallics **2002,** *21,* 4750−4755

Density Functional Theory Studies of Titanium-Catalyzed Hydroboration of Olefins

Dan Liu and Zhenyang Lin*

Department of Chemistry and Open Laboratory of Chirotechnology of the Institute of Molecular Technology for Drug Discovery and Synthesis,[†] The Hong Kong University of Science and Technology, Clear Water Bay, Kowloon, Hong Kong

Received April 23, 2002

The B3LYP method of density functional theory is used to study the hydroboration reaction of olefins catalyzed by $Cp_2Ti(HBcat')$. The favorable pathway is where the active species $Cp_2Ti(HBcat')$ initially coordinates an olefin to form a structural intermediate having a five-membered ring with a Ti−H−B bridging unit. B−H bond cleavage then occurs to allow the reductive elimination to form alkylboronate ester as the main product. Calculations show that from the B−H cleavage species the β-hydride elimination leading to the formation of side products, vinylboronate ester, is also competitive. Ti−O coordination is found to be the main reason for the lowering of the barrier of reductive elimination to form the main product, alkylboronate ester. The related olefin hydrogenation process has also been studied.

Introduction

In 1996, Hartwig and co-workers discovered a new and interesting titanocene bis(borane) σ-complex, $Cp_2Ti(\eta^2\text{-HBcat})_2$.[1] Further studies showed that the σ-complex and their analogues containing substituted catecholborane ligands display high catalytic activity for hydroboration of vinylarenes and other olefins.[2−5] Mechanistic studies (see Scheme 1)[4] revealed that the catalyst first dissociates one HBcat′ ligand. The fragment formed by the dissociation coordinates alkene to give a complex containing a Ti-η^2-HBcat′ unit. Reductive elimination from the complex gives anti-Markovnikov hydroborated (alkylboronate ester) products. In addition to the hydroborated products, side products such as vinylboronate ester and hydrogenation species have also been generated. The vinylboronate ester product is believed to be generated through β-hydride elimination from the complex.[4] Typical examples are given in Scheme 2.[4] One can see that both the catalytic and stoichiometric reactions shown in Scheme 2 give the hydroborated species as the main product. The hydrogenation species and vinylboronate ester are the side products.

In view of the interesting catalytic process, we feel it is necessary to theoretically study in more detail the reaction mechanism. In this paper, we report our theoretical calculations on the proposed reaction mechanism. We also attempt to understand the relevant β-hydride elimination process and how the hydrogenation species are generated in the catalytic process.

Scheme 1

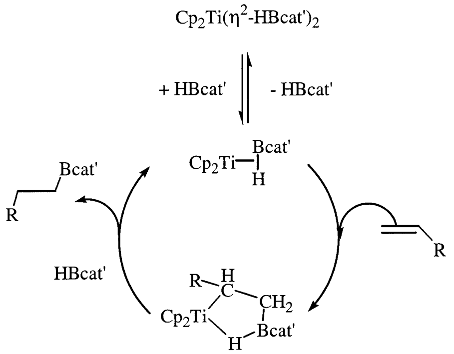

Scheme 2

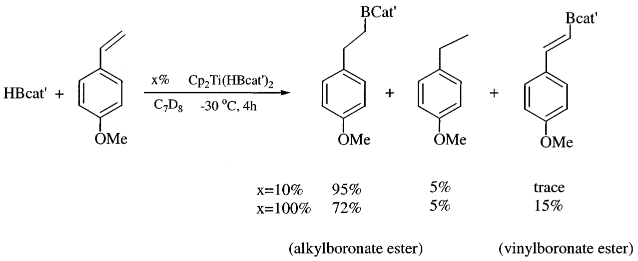

Unlike hydroboration reactions catalyzed by late transition metal complexes such as the Wilkinson's catalyst ($Rh(PR_3)_3Cl$), hydroboration reactions catalyzed by titanium complexes have not yet been studied theoretically. The extensive experimental[6−11] and theoretical[12−14]

[†] The University Grant Committee Area of Excellence Scheme (Hong Kong).

(1) Hartwig, J. F.; Muhoro, N.; He, X. M.; Eisenstein, O.; Bosque, R.; Maseras, F. *J. Am. Chem. Soc.* **1996**, *118*, 10936.

(2) He, X. M.; Hartwig, J. F. *J. Am. Chem. Soc.* **1996**, *118*, 1696.

(3) Muhoro, N.; He, X. M.; Hartwig, J. F. *J. Am. Chem. Soc.* **1999**, *118*, 5033.

(4) Muhoro, N.; Hartwig, J. F. *Organometallics* **2000**, *19*, 30.

(5) Pender, M. J.; Wideman, T.; Carroll, P. J.; Sneddon, L. G. *J. Am. Chem. Soc.* **1998**, *120*, 9108.

(6) Männing, D.; Nöth, H. *Angew. Chem., Int. Ed. Engl.* **1985**, *24*, 878.

(7) Burgess, K.; Ohlmeyer, M. *J. Chem. Rev.* **1991**, *91*, 1179.

(8) Evans, D. A.; Fu, G. C.; Hoveyda, A. H. *J. Am. Chem. Soc.* **1992**, *114*, 6671.

(9) Beletskaya, I.; Pelter, A. *Tetrahedron* **1997**, *53*, 4957.

(10) Burgess, K.; van der Donk, W. A.; Westcott, S. A.; Marder, T. B.; Baker, R. T.; Calabrese, J. C. *J. Am. Chem. Soc.* **1992**, *114*, 6671.

(11) Hayashi, T.; Matsumoto, Y.; Ito, Y. *J. Am. Chem. Soc.* **1989**, *111*, 3426.

10.1021/om020326b CCC: $22.00

studies show that the Rh(I)-catalyzed hydroboration reactions have very different reaction mechanisms when compared to the reactions catalyzed by early transition metals.[15−19] The studies here will provide more insights into the understanding of the different mechanisms.

Computational Details

On the basis of the fact that the Becke3LYP (B3LYP) method[20] can well describe the properties of transition metal compounds, all the geometries have been optimized using this method. The HBcat′ and *p*-methoxystyrene compounds are modeled by $HB(OH)_2$ and $H_2C{=}CH_2$ for computational simplicity, respectively. The effective core potentials of Hay and Wadt with double-ξ valence basis sets[21] (LanL2DZ) are used to describe Ti, while the 6-31G basis set is used for all other atoms. Polarization functions are added for the B atom (ξ(d) = 0.388) and for those H atoms (ξ(p) = 1.1) directly bonded to the transition metal. The frequency analysis has been performed for all calculated structures to confirm their characteristics as minima or transition states. All calculations are performed using the Gaussion 98 software package.[22]

To test the accuracy of the basis set used in our calculations, we performed single-point energy calculations for structures **1a**, **TS1a**, **2a-1**, **TS2a-3**, and **TS′2a** using a much large basis set which includes f polarization functions[23] (i.e., Lanl2dz + f) for Ti and 6-311G** for all other atoms. With the large basis set, the relative energies of **1a**, **TS1a**, **2a-1**, **TS2a-3**, and **TS′2a** are 0.0, 5.7, 1.1, 8.5, and 10.7, kcal/mol, respectively. In comparison to the relative energies obtained with the small basis set, which are shown in Figure 1, we can conclude that the effect of basis sets is not very important in the systems studied. Similarly, we used the five structures to test the solvent effect by employing the Onsager model reaction field calculations available in the Gaussian 98 package. The solvent used in the calculations is toluene. The relative energies including the solvent effect are 0.0, 5.4, 0.6, 7.8, and 9.8 kcal/mol for **1a**, **TS1a**, **2a-1**, **TS2a-3**, and **TS′2a**, respectively. Again, the solvent effect is also very small because toluene used in the experiments does not have a large dipole moment.

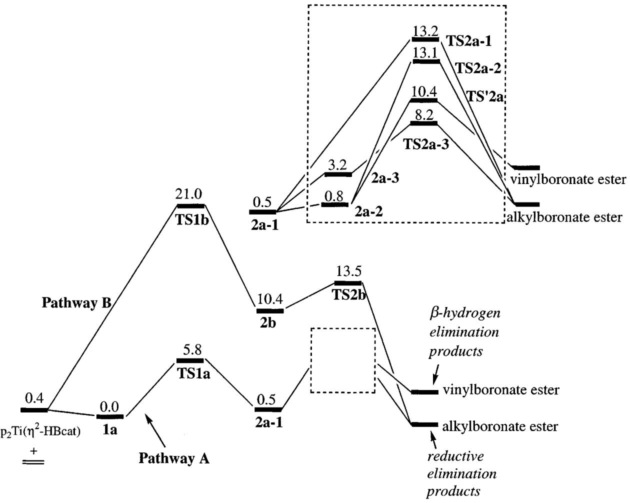

Figure 1. Potential energy profiles of pathways A and B. The relative reaction energies are in kcal/mol.

Results and Discussion

Catalyzed Hydroboration of Olefins. Mechanistic studies[3,4] showed that the $Cp_2Ti(\eta^2\text{-HBcat}')$ fragment is the active species in the catalytic process. The coordination of olefin to the active species is believed to be the first step in the hydroboration reactions. With the active species, the olefin ligand can approach the Ti center from two directions (see Scheme 3). Calculations show that when the olefin ligand approaches the Ti center from the Bcat′ side (pathway A), an intermediate structure **1a** having a bridging hydride unit is obtained. However, when the olefin ligand approaches the Ti center from the hydrogen side (pathway B), a transition state **TS1b** is found. In pathway A, the intermediate structure **1a** undergoes H−B bond cleavage to generate the $Cp_2Ti(Bcat')(CH_2CH_3)$ complex **2a** through the transition state **TS1a**. From the **2a** complex, competitive processes of a reductive elimination and a β-hydride elimination proceed to form the akylboronate ester and vinylboronate ester products, via the **TS2a** and **TS′2a** transition states, respectively. Very different from pathway A involving the direct formation of the intermediate structure **1a**, in pathway B, the olefin coordination with the active species $Cp_2Ti(\eta^2\text{-HBcat}')$ forms the $Cp_2Ti(Bcat')(CH_2CH_3)$ intermediate **2b** via the **TS1b** transition state. Intermediate **2b** then undergoes a reductive elimination to generate the alkylboranate ester products via the **TS2b** transition state.

The calculated energy profiles based on Scheme 3 are shown in Figure 1. Energetically, pathway A is much more favorable. The B−H bond cleavage from the intermediate **1a** requires a barrier of 5.8 kcal/mol, leading to the formation of **2a-1**. Interestingly, the intermediate **1a** has a stability similar to that of the B−H cleaved structure **2a-1**. Examining the structural change related to the cleavage process (see Figure 2), we can see that the stability of **2a-1** is gained through the strengthening of the B−C interaction together with the release of ring strain in compensation for the loss of the B−H interaction.

After the formation of **2a-1** through B−H bond cleavage in the intermediate structure **1a**, three possible reaction routes are found. A direct reductive elimination

---

(12) Musaev, D. G.; Mebel, A. M.; Morokuma, K. *J. Am. Chem. Soc.* **1994**, *116*, 10693.

(13) Dorigo, A. E.; Schleyer, P. v. R. *Angew. Chem., Ed. Engl.* **1995**, *34*, 115.

(14) Widauer, C.; Crützmacher, H.; Ziegler, T. *Organometallics* **2000**, *19*, 2097.

(15) Erker, G.; Noe, R.; Wingbermühle, D.; Peterson, J. L. *Angew. Chem., Int. Ed. Engl.* **1993**, *32*, 1213.

(16) Motry, D. H.; Smith, M. R. *J. Am. Chem. Soc.* **1995**, *117*, 6615.

(17) Lantero, D. R.; Ward, D. L.; Smith, M. R. *J. Am. Chem. Soc.* **1997**, *119*, 9699.

(18) Lantero, D. R.; Miller, S. L.; Cho, J. Y.; Ward, D. L.; Smith, M. R. *Organometallics* **1999**, *18*, 235.

(19) Kulkarni, S. A.; Koga, N. *THEOCHEM* **1999**, *461−462*, 297.

(20) Becke, A. D. *J. Chem. Phys.* **1993**, *98*, 5648. (b) Miehlich, B.; Savin, A.; Preuss, H. *Chem. Phys. Lett.* **1989**, *157*, 200. (c) Lee, C.; Yang, W. T.; Parr, G. *Phys. Rev. B* **1988**, *37*, 785.

(21) Hay, P. J.; Wadt, W. R. *J. Chem. Phys.* **1985**, *82*, 299.

(22) Frisch, M. J.; Trucks, G. W.; Schlegel, H. B.; Scuseria, G. E.; Robb, M. A.; Cheeseman, J. R.; Zakrzewski, V. G.; Montgomery, J. A., Jr.; Stratmann, R. E.; Burant, J. C.; Dapprich, S.; Millam, J. M.; Daniels, A. D.; Kudin, K. N.; Strain, M. C.; Farkas, O.; Tomasi, J.; Barone, V.; Cossi, M.; Cammi, R.; Mennucci, B.; Pomelli, C.; Adamo, C.; Clifford, S.; Ochterski, J.; Petersson, G. A.; Ayala, P. Y.; Cui, Q.; Morokuma, K.; Malick, D. K.; Rabuck, A. D.; Raghavachari, K.; Foresman, J. B.; Cioslowski, J.; Ortiz, J. V.; Stefanov, B. B.; Liu, G.; Liashenko, A.; iskorz, P.; Komaromi, I.; Gomperts, R.; Martin, R. L.; Fox, D. J.; Keith, T.; Al-Laham, M. A.; Peng, C. Y.; Nanayakkara, A.; Gonzalez, C.; Challacombe, M.; Gill, P. M. W.; Johnson, B.; Chen, W.; Wong, M. W.; Andres, J. L.; Gonzalez, C.; Head-Gordon, M.; Replogle, E. S.; Pople, J. A. *Gaussian 98 (Revision A.7)*; Gaussian, Inc.: Pittsburgh, PA, 1998.

(23) Ehlers, A. W.; Bohme, M.; Dapprich, S.; Gobbi, A.; Hollwarth, A.; Jonas, V.; Kohler, K. F.; Stegmann, R.; Veldkamp, A.; Frenking, G. *Chem. Phys. Lett.* **1993**, *208*, 111.

Scheme 3

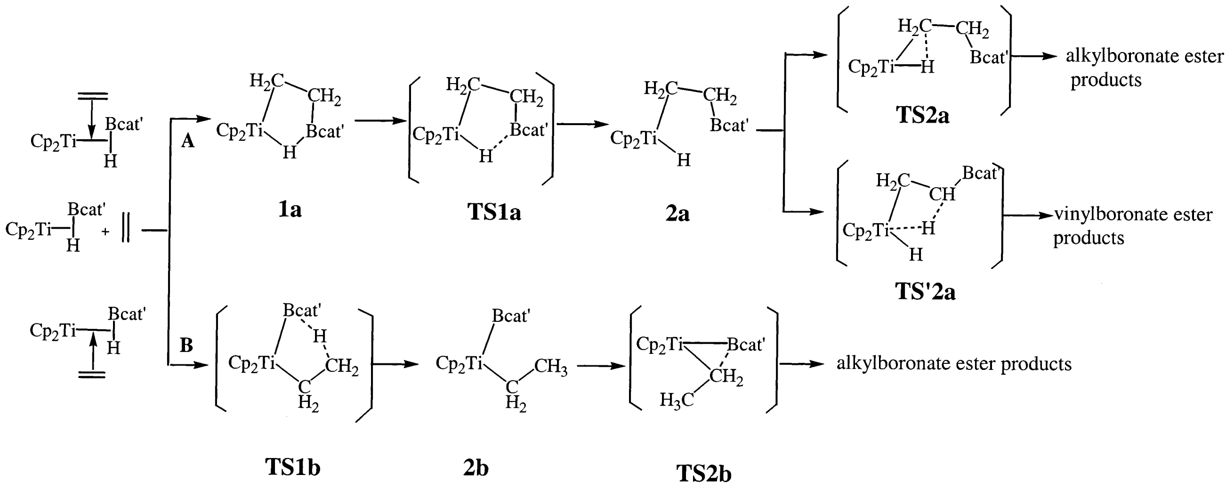

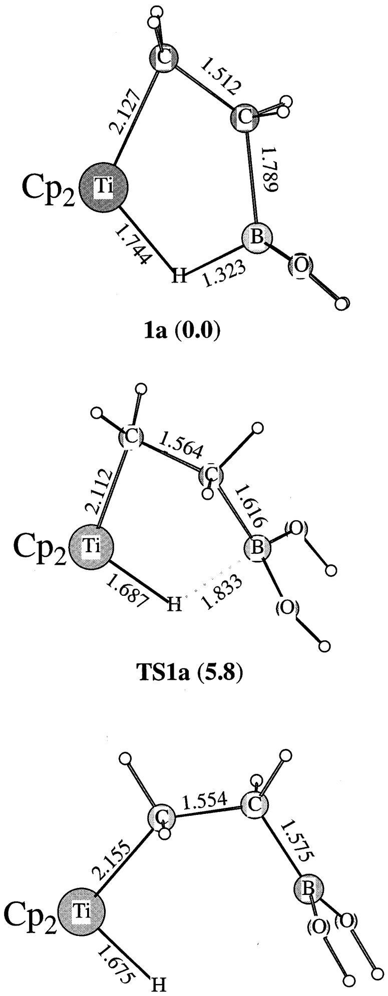

1a (0.0)

TS1a (5.8)

2a-1 (0.5)

Figure 2. Optimized structures involved in the B−H cleavage in pathway A. The relative energies are in kcal/mol. The bond distances and angles are in angstroms and degrees, respectively. For clarity, the atom positions of the two Cp ligands are not shown.

of alkylboronate from **2a-1** can occur through the transition state **TS2a-1**. The barrier for the elimination is calculated to be 12.7 kcal/mol, which is the highest one in pathway A. Figure 3 shows the structural

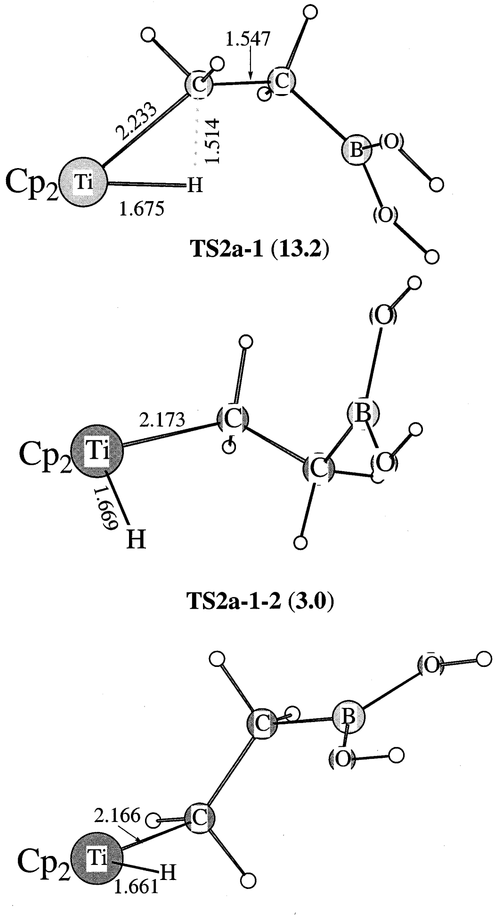

TS2a-1 (13.2)

TS2a-1-2 (3.0)

TS2a-1-3 (4.3)

Figure 3. Transition state structures in the reductive elimination of **2a-1** in the formation of alkylboronate ester and in the isomerizations of **2a-1** to **2a-2** and to **2a-3**. The relative energies are in kcal/mol. The bond distances and angles are in angstroms and degrees, respectively. For clarity, the atom positions of the two Cp ligands are not shown.

changes from **2a-1** to **TS2a-1**. The significant change is related to the H−Ti−C angle, which is reduced by moving the Ti−H bond toward the Ti−C bond. Alternatively, **2a-1** can isomerize via the **TS2a-1-2** and **TS2a-1-3** transition states (see Figure 3) through C−C

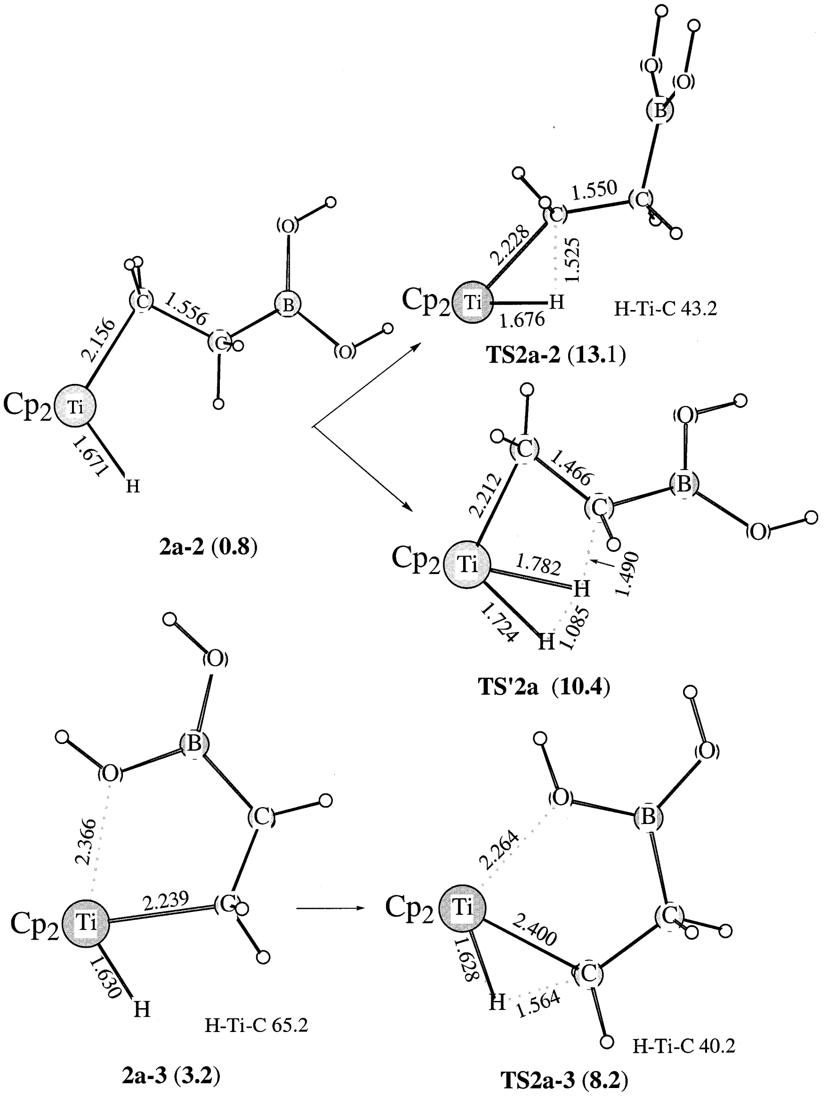

Figure 4. Optimized structures involved in the reductive elimination of isomers **2a-2** and **2a-3** and the β-hydride elimination of isomer **2a-2** in pathway A. The relative energies are in kcal/mol. The bond distances and angles are in angstroms and degrees, respectively. For clarity, the atom positions of the two Cp ligands are not shown.

and Ti–C bond rotations, respectively, giving **2a-2** and **2a-3** (see Figure 4). The rotational barriers are all small.

Similar to **2a-1**, isomer **2a-2** can also undergo a direct reductive elimination of alkylboronate. The calculations again show a high reaction barrier of 12.3 kcal/mol (see Figure 1). The relevant structural changes from **2a-2** to **TS2a-2** are also similar to those shown in the reductive elimination process of **2a-1**. Apart from the direct reductive elimination, isomer **2a-2** is also likely to undergo a β-hydride elimination, which gives the vinylboronate product, because one of the β-hydrogens in this structure is close to the metal center. The barrier for this elimination is calculated to be 9.6 kcal/mol, which is found to be the second most favorable reaction channel in pathway A. This low-energy and competitive β-hydride elimination process explains the formation of the vinylboronate side products in the hydroboration reaction observed experimentally.[4]

Quite different from the other two isomers, isomer **2a-3** introduces the additional Ti–O coordination (see Figure 4). The Ti–O coordination is possible because of the unsaturated 16-electron Ti metal center. However, the additional coordination apparently does not increase the stability of the complex. This is probably due to the more crowded coordination environment for the small-size Ti center as well as the strain of the five-membered ring. Indeed, the Ti–C bond (2.239 Å) is significantly lengthened due to the ring strain in comparison to those in the other two isomers (2.155–2.156 Å). Interestingly, Ti–O bond coordination makes the reductive elimination of alkylboronate ester from isomer **2a-3** most favorable. Reductive elimination is preferred over β-hydride elimination by 2.2 kcal/mol in the electronic energy (see Figure 1). When the entropy contribution is considered, the reductive elimination is still preferred but by a mere 0.3 kcal/mol in free energy (5.0 versus 5.3 kcal/mol). Here, one may question that the 0.3 kcal/mol difference is too small to distinguish the reaction preference when the entropy contribution is included. Careful examination of the entropy contribution to **2a-2** and **2a-3** revealed that **2a-2** is relatively lowered by 4.7 kcal/mol while **2a-3** is lowered only by 3.0 kcal/mol when the free energies are considered. In other words, the step from **2a-3** to **TS2a-3** (the reductive elimination) is an easier one in comparison to the step from **2a-2** to **TS′2a** (the β-hydride elimination). In view of the fact that

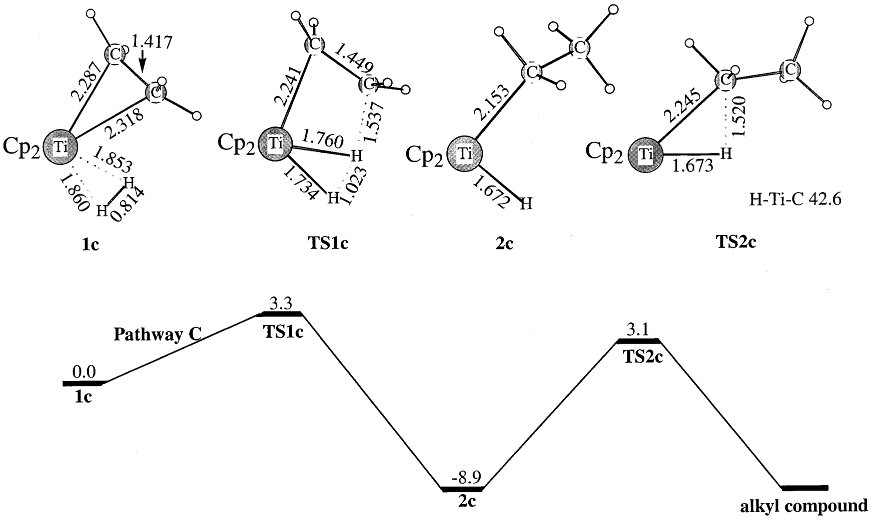

Figure 5. Potential energy profile and the optimized structures involved in the hydrogenation of olefins. The relative energies are in kcal/mol. The bond distances and angles are in angstroms and degrees, respectively. For clarity, the atom positions of the two Cp ligands are not shown.

TS2a-3 is still relatively lower than **TS′2a** in their relative free energies and the smaller barrier from **2a-3** to **TS2a-3**, we can conclude that the reductive elimination is more favorable even when the entropy contribution is included. Clearly, the Ti−O coordination significantly reduced the barrier of the reductive elimination step. This explains the alkylboronate ester as the main product formed in the catalyzed hydroboration reactions. It should be noted here that a similar Rh−O coordination was also found in the Rh-catalyzed hydroboration reactions.[14]

Very different from the favorable pathway A, pathway B directly forming the **2b** complex via the transition state **TS1b** is very unfavorable. These results suggest that the olefin substrates prefer to approach the metal center through the Bcat′ side, allowing the C−B bond formation. The preference of approaching the metal center from the Bcat′ side explains the regioselectivity observed experimentally in which anti-Markovnikov products were produced.[4] The steric repulsion interactions force the arenyl groups of vinylarene substrates away from the Bcat′ group (see Scheme 1).

Catalyzed Hydrogenation of Olefins. The discussions in the preceding section show that the β-hydride elimination from isomer **2a-2** is the second most favorable reaction in comparison to the reductive elimination from **2a-3**, which gives the main product, alkylboronate ester. Through the β-hydride elimination, a dihydrogen complex containing the vinylboronate ester $[Cp_2Ti(\eta^2\text{-}H_2)(H_2C{=}CHBcat')]$ is generated. From this dihydrogen complex, a ligand exchange reaction between the vinylboronate ester and olefin substrates can occur easily, leading to the formation of the side product, vinylboronate ester, as well as the olefin−dihydrogen complex **1c**. The claim of the easiness of the olefin exchange is supported by the small olefin dissociation energy calculated for $[Cp_2Ti(\eta^2\text{-}H_2)(H_2C{=}CHB(OH)_2)]$. The calculated dissociation energy is 13.6 kcal/mol. With the entropy contribution, the dissociation free energy (3.4 kcal/mol) is much smaller. The small olefin dissociation energy can be explained as follows. In $H_2C{=}CHB(OH)_2$, the stabilization of the π-bonding orbital by the "empty" p orbital of the boryl substituent weakens the coordination ability of the olefin bond. In addition, the formation of the stable Cp_2TiH_2 dihydride after the olefin dissociation may also promote the dissociation process. The olefin exchange reaction is expected to have an even smaller barrier because the dissociation energy is the upper limit for the exchange reaction. Therefore, the formation of **1c** makes the hydrogenation of olefin substrates possible. The hydrogenation process proceeds with the olefin insertion into the Ti−H bond followed by reductive elimination (see Figure 5). Energetic calculations show that the process is very favorable. The reaction barriers associated with the process are in the range 3.0−12.0 kcal/mol. These results are consistent with the experimental observation in which the olefin substrates are also hydrogenated.[4]

Comments on the Transition State Structures of the Studied Reductive Elimination Steps. TS2a-1 in Figure 3, **TS2a-2** in Figure 4, and **TS2c** in Figure 5 are the transition state structures of the studied reductive elimination steps discussed in the sections above. One may notice that these transition state structures involve a significant decrease in the H−Ti−C angle by moving the Ti−H bond toward the Ti−C bond and have unsymmetrical arrangements between the hydride and alkyl ligands. One normally expects that the large decrease of the H−Ti−C angles occurs by simultaneously moving the Ti−H and Ti−C bonds toward each other instead of moving the Ti−H bond only. To understand the structural feature of these transition state structures that involve the large angle changes, we consider complex Cp_2TiR_2 and its reductive elimination products CP_2Ti and R−R. Examining their molecular orbital structures (see Figure 6), we can see that a symmetric path in the reductive elimination of R−R from Cp_2TiR_2 is symmetry-forbidden for such a 16-e species because the two Ti−R σ bonds transform as a′ + a″, while the d orbital accommodating the two d electrons of Cp_2Ti has the a′ irreducible representation and the R−R σ bond is also a′ if we imagine a mirror plane bisecting the R−Ti−R angle. Because of the symmetry-forbidden nature for such a 16-e Cp_2TiR_2 complex, it is not too surprising that the studied reductive elimination reaction steps involve asymmetric

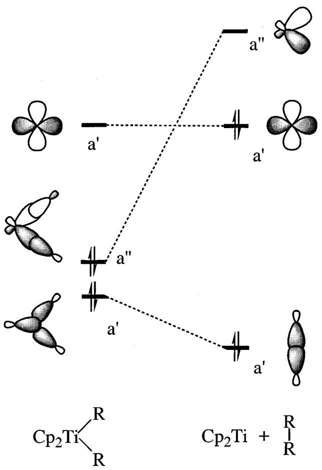

Figure 6. Schematic illustration of the molecular orbitals involved in the reductive elimination of R−R from Cp_2TiR_2. The irreducible representations are based on the assumption of a mirror plane bisecting the R−Ti−R angle.

bending in their reaction paths. Calculations show that for a considered complex the transition state structure is the one where the Ti−H bond approximately overlaps with the plane formed by the metal center and the centers of the two Cp rings. In these transition state structures, the Ti−C bonds are moderately weakened. The motion of Ti−H toward Ti−C instead of Ti−C toward Ti−H may be related to the fact that hydrogen is more labile than alkyl.

Summary

In this paper, the reaction mechanism of the Ti-catalyzed hydroboration of olefins has been theoretically investigated. Our calculations support the proposed mechanism[4] that the favorable reaction pathway involves olefin insertion into the Ti−B bond, giving a structural intermediate **1a**, followed by B−H bond cleavage from the intermediate to form the alkyl-hydride complex **2a** and then reductive elimination of **2a**. The reductive elimination step is found to be rate-determining. The competitive β-hydride elimination that gives the vinylboronate ester side product is based on an isomer of the alkyl-hydride complex **2a** formed through the B−H bond cleavage. The hydrogenated side product is obtained through the formation of the olefin-dihydrogen complex **1c**, which results from the β-hydride elimination. Through our calculations, we also found that the Ti−O coordination plays a crucial role in reducing the reaction barrier of the rate-determining step. Here, the oxygen atom is from the Bcat′ group. Without the coordination, the calculations predict that the β-hydride elimination, which gives vinylboronate corresponding to the borylation of C−H at the terminal olefin carbon, would become the most favorable process. This important prediction can be tested if 9-borabicyclo-[3.3.1]nonane (9-BBN), which does not contain O-donor atoms, is used instead of HBcat′.

In comparison to late transition metal-catalyzed hydroborations, the Ti-catalyzed process shows that the strong tendency to form the five-membered ring structural intermediate through the C−B interaction leads to the exclusive formation of anti-Markovnikov products. For late transition metal-catalyzed processes, oxidative addition of the HB bond to a metal center gives the hydroboryl active species, which allow more modes for olefin coordination.[12−14] More olefin coordination modes complicate the product formation because the insertion of olefins to both the metal boryl and metal-hydride bonds is possible.[7−10]

Acknowledgment. This work was supported by the Research Grants Council of Hong Kong and the University Grants Committee of Hong Kong through the Area of Excellence Scheme (Aoe).

OM020326B